



## Enantioselective hydrogenation of 1-phenyl-1,2-propanedione over Pt on immobilized cinchonidine on $\gamma$ -Al<sub>2</sub>O<sub>3</sub> catalysts



Cristian H. Campos <sup>a</sup>, Cecilia Torres <sup>a</sup>, José L.G. Fierro <sup>b</sup>, Patricio Reyes <sup>a,\*</sup>

<sup>a</sup> Edmundo Larenas 129/Departamento de Fisicoquímica, Facultad de Ciencias Químicas, Universidad de Concepción, Concepción, Chile

<sup>b</sup> c/Marie s/n Cantoblanco 28049/Instituto de Catálisis y Petroleoquímica, CSIC, Departamento de Reactividad y Estructura, Madrid, Spain

### ARTICLE INFO

#### Article history:

Received 23 February 2013

Received in revised form 18 June 2013

Accepted 25 June 2013

Available online 4 July 2013

#### Keywords:

Heterogenization

Platinum

Cinchonidine

1-Phenyl-propane-1,2-dione

Immobilized heterogeneous catalyst

### ABSTRACT

Chirally modified  $\gamma$ -Al<sub>2</sub>O<sub>3</sub> containing different amounts of cinchonidine were prepared by the chemical modification of cinchonidine with trimethoxysilane (TMS-CD). These solids were used as support of Pt catalysts containing 1 wt% Pt by chemical reduction of the hexachloroplatinic acid with H<sub>2</sub> at 25 °C and 40 bar. The characterization was carried out by elemental analysis of C, H and N, TG, DRIFT, NMR <sup>13</sup>C and <sup>29</sup>Si on solid state, N<sub>2</sub> adsorption-desorption at 77 K, XDR, XPS and TEM. The catalytic activity was evaluated in the hydrogenation of 1-phenyl-propane-1,2-dione in a batch reactor at 298 K and 40 bar. The effect of H<sub>2</sub> pressure, concentration substrate, catalyst mass, solvents effect and recycles, of the catalyst with the major enantiomeric excess was studied. It was found that all catalysts were active in the reaction being the enantiomeric excess of the target product, 1-R-phenyl-1-hydroxy-2-propanone in the range 30–44% and the best catalyst is that supported on  $\gamma$ -Al<sub>2</sub>O<sub>3</sub> with a nominal content of 5 wt% TMS-CD. The results obtained in this study confirm that the variation of reaction conditions show a dependence on the activity and enantioselectivity for substrate adsorption in the metal active sites. In the solvent effect, enantiomeric excess decreased non-linearly with an increasing solvent dielectric and we could be attributed to the interactions between solvents and TMS-CD in the surface. In the recycles studies enantiomeric excess was achieved as 40% even after 3rd reuse with a slight loss in activity and enantiomeric excess.

© 2013 Elsevier B.V. All rights reserved.

## 1. Introduction

The need to develop effective catalysts for enantioselective synthesis is becoming important as regulatory authorities increasingly insist that a single enantiomer of a racemic bioactive compound must be used in pharmaceuticals or agrochemicals [1–4]. In the production of optically pure chemicals (e.g., pharmaceuticals, agrochemicals, fragrances, sweeteners, etc.), the use of heterogeneous catalysis, which combine easy catalyst separation and lower preparation costs (compared to chiral homogeneous catalysts), is particularly attractive. A successful and commonly applied strategy in heterogeneous enantioselective catalysis is the modification of the metal active site by a strongly adsorbing chiral organic compound, termed as modifier or inducer [2,3,5–7]. Cinchona alkaloids are an important class of natural chiral compounds that have been used in different fields, e.g., as pharmaceuticals and chiral resolving agents for separation of optical isomers, and in catalytic applications as catalysts and as chiral auxiliaries. The most studied application of cinchona alkaloids is their

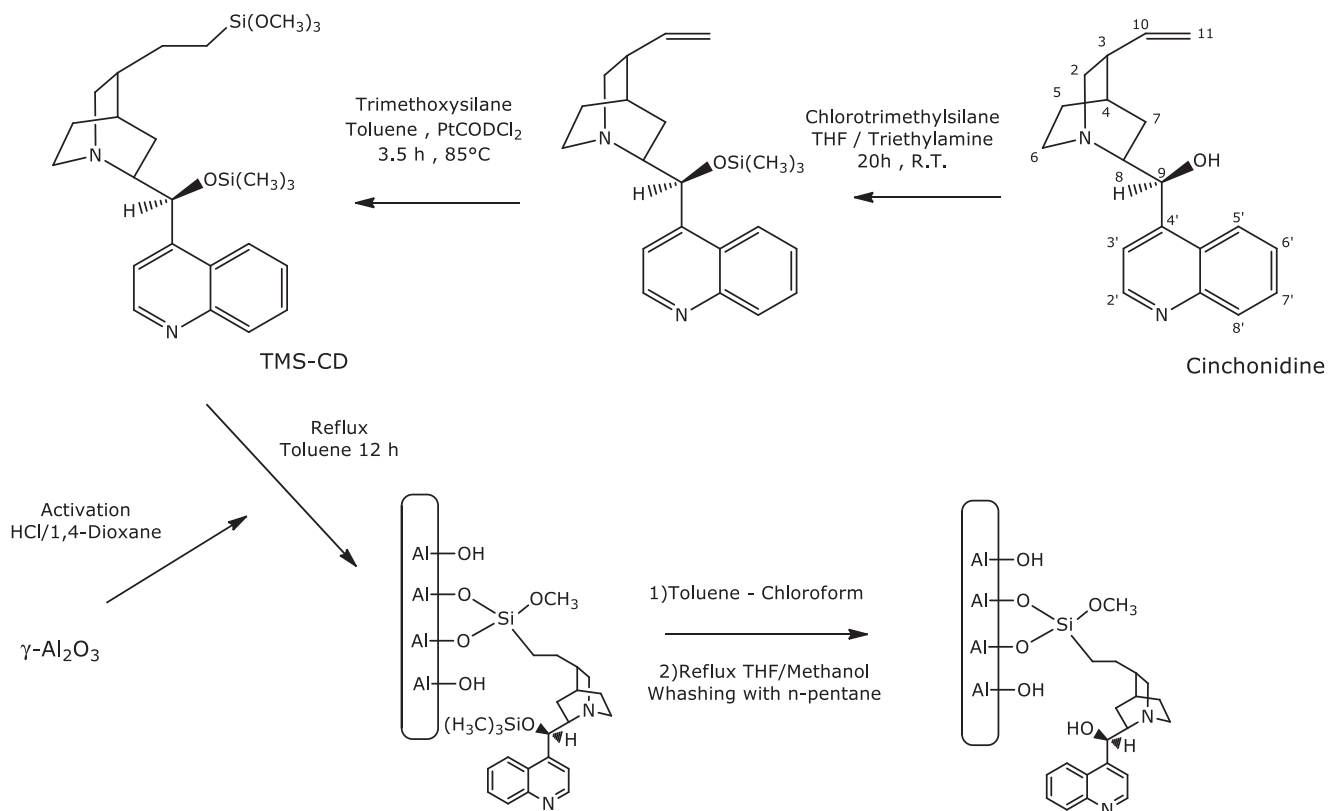
use as chiral inducers in heterogeneous Pt and Pd catalysts for enantioselective hydrogenation of many substrates with a moderate (40–60%) [8–10] and high enantiomeric excess (80–95%) [11–13].

The commercial application of such systems obviously requires an effective method of catalyst recovery and re-use, because of both economic and environmental reasons. Several methods for the recycling of chiral catalysts have been described. The immobilization of transition metal complexes on solid supports for selective reactions in fine chemistry has been mainly performed over silica based materials [14–17]. The general trend is to functionalize the support material by performing a hydroxylation treatment to obtain a more reactive and hydrophilic surface. The surface of the support has been modified using building-blocks as alkylchlorosilanes, alkoxy silanes, and amines [18–23].

The focus of the present study is to create a simple and efficient process by direct tethering of modified cinchonidine (CD) molecule within mesoporous  $\gamma$ -Al<sub>2</sub>O<sub>3</sub>. For this purpose, CD was functionalized with trimethoxysilane (TMS-CD). The anchoring process takes place by the reaction between Al–OH groups on the support surface and alkoxy silane groups in the TMS-CD. Active phase deposition was performed by *in situ* precursor reduction employing high H<sub>2</sub> pressure in an autoclave. The obtained catalysts were tested in

\* Corresponding author. Tel.: +56 41 203353; fax: +56 41 2245974.

E-mail addresses: [ccampos@udec.cl](mailto:ccampos@udec.cl) (C.H. Campos), [preyes@udec.cl](mailto:preyes@udec.cl) (P. Reyes).

**Scheme 1.** Synthetic route for modified supports.

the enantioselective hydrogenation of 1-phenyl-1,2-propanedione (PPD).

## 2. Experimental

### 2.1. Activation of $\gamma\text{-Al}_2\text{O}_3$

The surface activation was carried out in a round-bottom flask in which 3.0 g of  $\gamma\text{-Al}_2\text{O}_3$  with 24 mL of 1,4-dioxane and 3 mL HCl 3.1 mol/L were mixed. This system was stirred for 30 min at 353 K, filtered, and dried under vacuum for 4 h at 393 K.

### 2.2. Preparation of modified CD

The modification of CD and its later hydrosilation were done as reported in a previously work [24]. An ice-cooled solution of CD in THF containing TEA was added dropwise to the chlorotrimethylsilane. The reaction mixture was stirred for 20 h at room temperature and then for 2 h at 333 K. The product was extracted with chloroform and washed with water. The obtained product was hydrosylated using  $\text{PtCODCl}_2$  and trimethoxysilane at 313 K using toluene as solvent. The reaction mixture was stirred for 5 h at 363 K under a  $\text{N}_2$  atmosphere. Purification by flash chromatography (hexane-acetone-TEA 40:18:1).

### 2.3. Synthesis of modified $\gamma\text{-Al}_2\text{O}_3$

Five supports were prepared with different amounts of CD (1%, 5%, 10%, 15%, 20% in mass), simulating the CD fractions that are added in traditional systems. 2.0 g of activated  $\gamma\text{-Al}_2\text{O}_3$  and the necessary quantity of TMS-CD dissolved in toluene were deposited in a round-bottom flask, and the volume of the system was completed to 50 mL with solvent (see Scheme 1). The reaction was refluxed for 12 h and later filtered and washed two times with 40 mL toluene

and 20 mL chloroform. The solid was dried in a furnace for 1 h at 353 K. Later, the solid obtained was treated by refluxing it in a mixture methanol/THF for 20 h and was then washed with 100 mL of  $n\text{-pentane}$ . Finally, the solids were dried under vacuum for 4 h at 393 K. All the samples of modified supports were tabulated as  $\text{AlCD}(x)$ , where  $x$  is the nominal % in mass.

### 2.4. Catalyst preparation

The catalyst (1.0 g) was prepared at 1% Pt mass using the five modified supports and activated  $\gamma\text{-Al}_2\text{O}_3$ . These were labeled as 1%  $\text{Pt/AlCD}(x)$ , where  $x$ : 1–20. The methodology is analogous to that reported by Roucoux et al. [25]. The support plus the necessary quantity of  $\text{H}_2\text{PtCl}_6 \cdot 6\text{H}_2\text{O}$  and a stoichiometric quantity of NaOH 0.5 mol/L were added to a batch reactor equipped with a Teflon cup. The pressure was adjusted to 40 bar  $\text{H}_2$  for 2 h with constant magnetic stirring, obtaining the reduced supported metal. Later, the solid was filtered and washed to a constant pH and conductivity. Finally, it was dried in a vacuum oven at 373 K for 1 h and storage in a desiccator using  $\text{N}_2$  atmosphere previous to the catalytic test.

### 2.5. Characterization

Elemental analyses of C, H, and N were performed on a LECO CHNS-932 analyzer. TG studies were carried out in a Mettler Toledo Thermogravimetric TGA/SDTA 851 using an  $\text{O}_2$  flow of 25 mL/min and  $1^\circ/\text{min}$  to 298–1000 K. NMR spectra for  $^1\text{H}$  and  $^{13}\text{C}\{\text{H}\}$  were obtained on a Bruker AMX-300 spectrometer (300 MHz for  $^1\text{H}$ , 75 MHz for  $^{13}\text{C}$ ) using trimethylsilane as a standard; all the results obtained from the NMR of  $^1\text{H}$  and  $^{13}\text{C}$  were compared with the results reported by Leino et al. [26,27] in terms of the observed allocations and dislodged chemical signals. Solid-state  $^{13}\text{C}$  and  $^{29}\text{Si}$  CP NMR spectra were recorded at 100.6 and 79.49 MHz, respectively, using a Bruker AV 400 WB spectrometer. Diffuse reflectance

**Table 1**  
Elemental analysis of supports and catalysts synthesized.

Sample	C (%)	H (%)	N (%)	TMS-CD (wt%)	Yield <sup>a</sup> (%)
AICD(1)	1.19	1.43	0.07	0.9	92.9
1% Pt/AICD(1)	0.84	1.11	0.05	0.7	71.4
AICD(5)	3.59	2.28	0.33	4.7	94.3
1% Pt/AICD(5)	2.16	1.13	0.22	3.1	61.4
AICD(10)	5.42	2.58	0.56	8.0	79.3
1% Pt/AICD(10)	3.07	1.24	0.32	4.5	45.0
AICD(15)	5.87	2.55	0.61	8.7	57.6
1% Pt/AICD(15)	3.54	1.22	0.37	5.2	34.8
AICD(20)	6.11	2.66	0.67	9.6	47.5
1% Pt/AICD(20)	4.03	1.34	0.44	6.3	31.4

<sup>a</sup> Yield: (TMS-CD<sub>Real</sub>/TMS-CD<sub>Nominal</sub>) × 100%.

infrared fourier transform (DRIFT) spectra were carried out on a JASCO FT/IR-6300 spectrometer. XRD patterns were recorded on a RigakuD/max-2500 diffractometer with Cu K $\alpha$  radiation at 40 kV and 100 mA. N<sub>2</sub> adsorption–desorption isotherms at 77 K were performed on a Micromeritics ASAP 2010 apparatus. Specific surface areas were determined by the BET (Brunauer–Emmett–Teller) equation, using adsorption data in the relative pressure range of 0.05–0.3, and pore-size distributions were estimated using the BJH model. HR-TEM micrographs were obtained with HR-TEM Philips CM-200 STEM. Photoelectron spectra (XPS) were recorded using an Escalab 200 R spectrometer equipped with a hemispherical analyzer and using non-monochromatic Mg K $\alpha$  X-ray radiation ( $h\nu = 1253.6\text{ eV}$ ). The surface Pt/Al and N/Al atomic ratios were estimated from the integrated intensities of Pt 4f, Al 2p, C 1s, and N 1s lines after background subtraction and corrected by the atomic sensitivity factors [28]. The spectra were fitted to a combination of Gaussian–Lorentzian lines of variable proportion. The C 1s core-level of adventitious carbon at a binding energy (BE) of 284.9 eV was taken as an internal standard.

## 2.6. Catalytic activity

The catalytic assays of PPD hydrogenation were performed in a stainless steel, Parr-type batch reactor at a concentration of 0.01 mol/L of substrate using cyclohexane as a solvent and stirring at 700 rpm under 40 bar H<sub>2</sub> pressure. All further experiments were carried out in the absence of external mass transfer limitations. The used catalysts were in the form of fine powders (>30  $\mu\text{m}$ ) assuming negligible effect of pore diffusion limitations. In catalyst mass studies, the surface (PPD/Pt) molar ratio was varied, the concentration of PPD was kept constant and the mass of the catalyst was modified. Non-important difference obtained in initial velocity in the range of catalyst mass studied (0.01–0.07 g), because the reaction rate was proportional to the catalyst mass. These are indicating that gas–liquid and liquid–solid external mass transfer limitations were absent [42,44,51].

Analyses of reactants and products were followed by gas chromatography mass spectrometry using a GC-MS device (Shimadzu GCMS-QP5050) with chiral  $\beta$ -Dex 225, a 30-m column (Supelco), and helium as the carrier gas. The recycling assays were done by filtering the catalyst from the reaction medium. The filtered catalyst was washed three times consecutively with chloroform to clean the surface and then dried at 373 K for 24 h.

In relation to the selectivity of the catalysts, enantiomeric excess and regioselectivity have been defined as:

$$\text{ee}_{\text{CX}} (\%) = \frac{[\text{R}]_x - [\text{S}]_x}{[\text{R}]_x + [\text{S}]_x} \cdot 100 \quad \text{and} \quad \text{rs} = \frac{[\text{R}_{\text{C}1}] + [\text{S}_{\text{C}1}]}{[\text{R}_{\text{C}2}] + [\text{S}_{\text{C}2}]}$$

where [R] and [S] correspond to the concentration of the respective enantiomers, x is the number of the carbonyl group and in the case of rs, to the alcohols of the different carbonyl groups.

## 3. Results and discussion

### 3.1. Support syntheses and characterization

The total content of CD anchored on the surface was lower than the nominal content, and the decrease in the anchored amount became more significative as the nominal content of the inducer increased. Table 1 summarizes the elemental analysis of the supports. This effect can be explained by diffusion phenomena similar to that reported by Campos et al. [24]. Other species anchored on the surface of  $\gamma$ -Al<sub>2</sub>O<sub>3</sub> are (CH<sub>3</sub>)<sub>3</sub>Si—O—Al and CH<sub>3</sub>—O—Al, which were formed during the support modification [24]. Thus, our calculations were based on N (%), because it is the only vector of the real TMS-CD content anchored on  $\gamma$ -Al<sub>2</sub>O<sub>3</sub>.

The apparent loss of C (%) was studied using TG-O<sub>2</sub>. Fig. 1 shows the curves of loss mass as a function of the temperature for the different synthesized supports. Low quantity of OH groups on the surface of  $\gamma$ -Al<sub>2</sub>O<sub>3</sub> was observed. The mass loss is due to dehydroxylation. The heterogenized supports with TMS-CD display major mass loss attributed to the loss of organic matter [24].

Fig. 2 shows the DRIFT spectra of the synthesized supports. In the case of AlCD(0.0), an intense band around 3500–4000 cm<sup>-1</sup> corresponding to the vibration of the hydroxyl groups of activated  $\gamma$ -Al<sub>2</sub>O<sub>3</sub> was detected. As the TMS-CD began to anchor on the solid, the band decreased, and vibrations corresponding to the C—H bonds appeared at frequencies in the range between 2900 and 3000 cm<sup>-1</sup>. These bands increased in intensity along with the content of organic matter on the solid. A discreet band appeared between 1400 and 1500 cm<sup>-1</sup>, corresponding to vibrations of bonds of the type Si—CH<sub>3</sub> [29,30]. This band was attributed to the vibrations of trimethylsilane species (impurities) anchored to the surface of the support as verified by NMR of solids (displayed in Fig. 3).

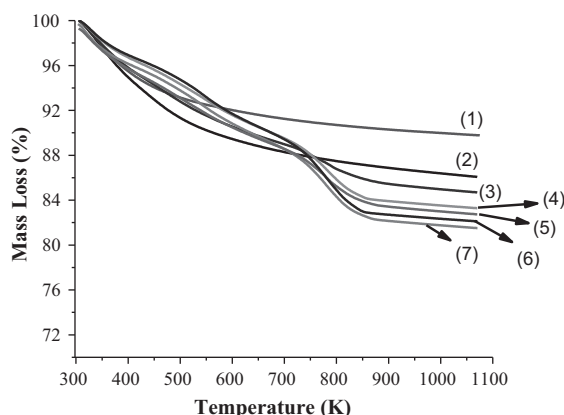


**Fig. 1.** TG curves for the synthesis supports. Conditions: O<sub>2</sub> atmosphere to 25 mL/min flow and temperatures 298–1000 K. (1)  $\gamma$ -Al<sub>2</sub>O<sub>3</sub>, (2) AlCD(0), (3) AlCD(1), (4) AlCD(5), (5) AlCD(10), (6) AlCD(15) and (7) AlCD(20).

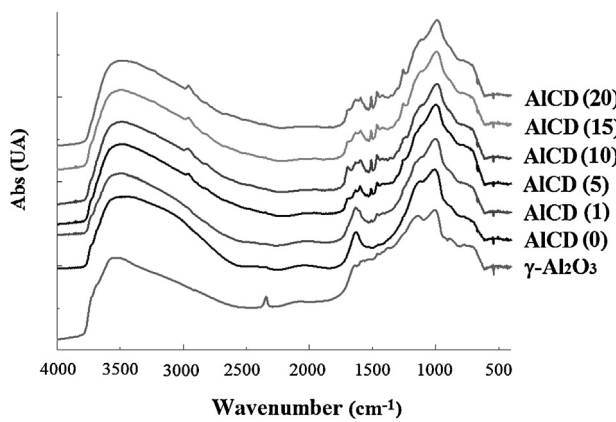


Fig. 2. DRIFT of the supports modified with TMS-CD.

**Table 2**

Physicochemical properties:  $S_{\text{BET}}$ , pore diameter and metallic nanoparticles diameter of 1 wt% Pt/AICD(x) catalysts.

Catalyst	$S_{\text{BET}}$ ( $\text{m}^2/\text{g}$ )	Average pore diameter (nm)	$d_p$ TEM* (nm)
1% Pt/AICD(0.0)	210	7.8	10
1% Pt/AICD(0.5)	181	7.8	8.3
1% Pt/AICD(2.5)	176	7.6	4.8
1% Pt/AICD(5.0)	173	6.9	4.1
1% Pt/AICD(7.5)	169	6.8	3.9
1% Pt/AICD(10)	159	6.5	3.3

Fig. 3(a) shows an unusual band between  $-1.0$  and  $-2.0$  ppm corresponding to Si–CH<sub>3</sub> species. All the samples display a significant increase in the characteristic bands of the aromatic and aliphatic zones, in direct relationship with the TMS-CD content in the samples. Fig. 3(b) shows the NMR <sup>29</sup>Si for the AICD(20). A characteristic signal of a Si atom monocoordinated with an O atom from the Al<sub>2</sub>O<sub>3</sub> network (13 ppm) was observed, and it was attributed to Si impurities. Since the AICD(20) possesses the major TMS-CD content on the surface, the characteristic anchoring signals of the T<sup>2</sup> and T<sup>3</sup> type at  $-50$  and  $-80$  ppm were detected [18,29–31].

Table 2 displays the surface areas and pore size distributions of AICD(x) supports. The analysis of N<sub>2</sub> adsorption–desorption isotherms and  $S_{\text{BET}}$  shows that all the solids were mesoporous and had a type IV hysteresis cycle, corresponding to cylindrical pores. Moreover, all of them displayed monomodal pore-size distributions. This information allows us to infer that as the TMS-CD content increased on the supports, the values of surface area, pore volume,

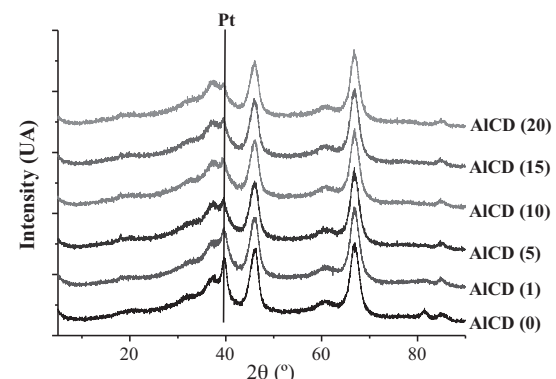


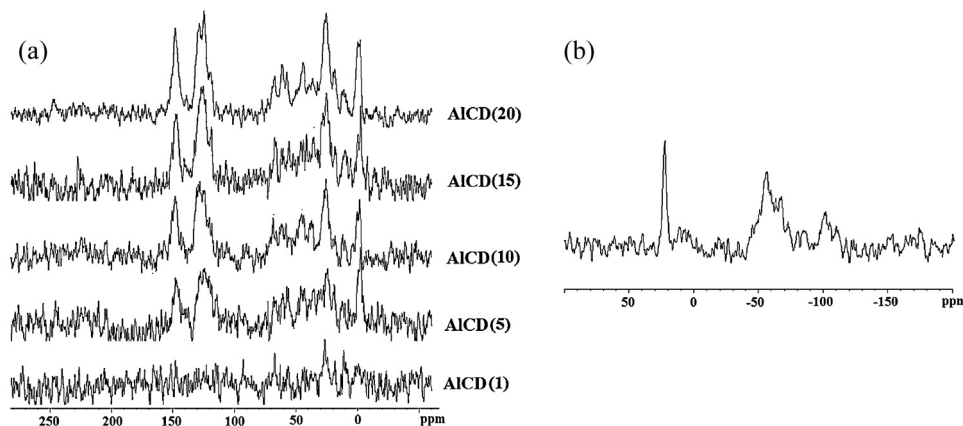
Fig. 4. XRD patterns of the catalysts synthesized on modified supports.

and pore size dropped due to the anchoring of the organic molecule on the surface.

### 3.2. Catalyst synthesis and characterization

During the Pt nanoparticles synthesis H<sub>2</sub> oxidizes to H<sup>+</sup> and provides an acid medium that could interact with the basic N of the quinuclidine ring of the anchored inducer, the stoichiometric addition of NaOH to the synthesis system allowed us to obtain a neutral medium at the end of the reduction process. Table 1 summarizes the values obtained from the surface concentration of the inducer on the catalysts. A decrease in the TMS-CD content was observed and it was attributed to the catalyst preparation conditions, which involved a slight leaching of the inducer and the corresponding impurities, as discussed in previous work [24].

The DRIFT spectra and N<sub>2</sub> adsorption–desorption isotherms of the supports and catalysts did not show significant differences and the crystalline nature of the active phase dispersed in the support was studied by XRD (Fig. 4). The characteristic Pt diffraction lines in the region of  $2\theta \sim 40^\circ$  were detected. The metal particle size shown in Table 2 was determined by HR-TEM and can be seen in the micrograph shown in Fig. 5. The catalyst prepared on the activated support displayed large particle sizes, reaching approximately 10 nm, and a wide distribution of particle size values. The average metal particle size in those samples displays an inverse relationship with TMS-CD content. The organic molecule provided stability to the Pt cluster formed during the metal reduction, thereby allowing the formation of smaller-size agglomerates.

Fig. 3. NMR of the supports modified with TMS-CD. (a) <sup>13</sup>C and (b) <sup>29</sup>Si (CP).

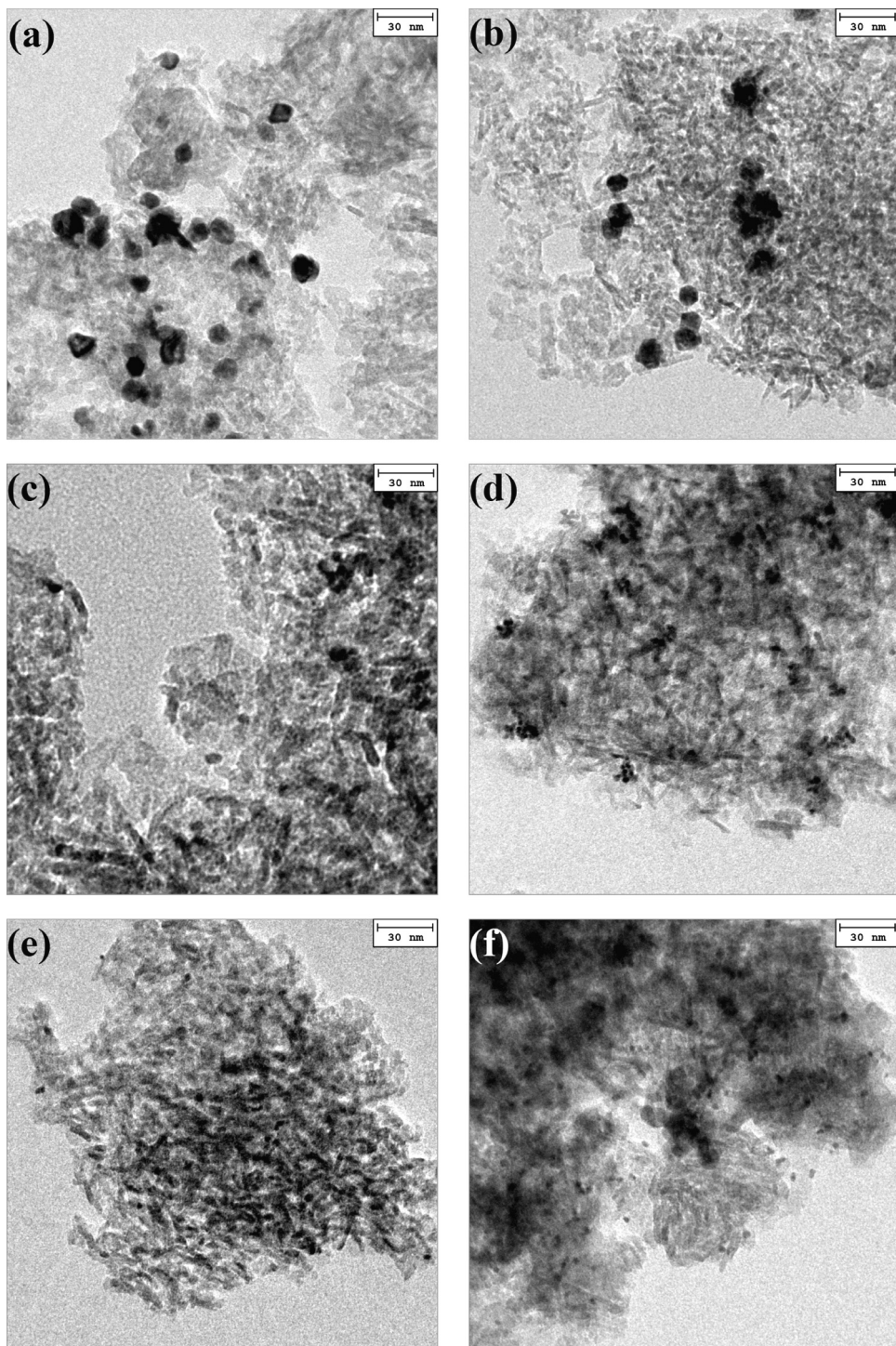


**Fig. 5.** HR-TEM micrograph of the catalysts 1 wt% Pt supported on the modified  $\gamma$ - $\text{Al}_2\text{O}_3$ : (a) AlCD(0), (b) AlCD(1), (c) AlCD(5), (d) AlCD(10), (e) AlCD(15) and (f) AlCD(20).

Given these conditions of catalyst preparation, a preferential deposition toward immobilized TMS-CD sites was expected.

The chemical changes in the platinum particles were also investigated by XPS. [Table 3](#) gives the Pt 4d<sub>5/2</sub> BEs for all of the catalysts under study, with the corresponding contribution to the overall signal in parentheses. It is interesting to observe the appearance of a band centered at around 317.0 eV in all the samples, which is indicative of the presence of  $\text{Pt}^{\delta+}$  character indicating a strong platinum–support interaction, in agreement with results of Corro et al. [[32](#)]. With greater TMS-CD contents, the band of species of the

type  $\text{Pt}^{\delta+}$  became slightly more intense, mainly due to the interaction of the nanoparticles with the N atoms of the inducer [[33,34](#)]. An increment in the Pt/N surface ratio due to the surface coverage of the support by TMS-CD was detected. Nonetheless, the Pt/Al ratio increased along with the TMS-CD content at the surface, as shown by EA and DRIFT ([Table 1](#) and [Fig. 2](#)). The decline of the atomic ratio of Pt/N in the catalysts led us to assume that as the TMS-CD content increased on the surface. Nanoparticles were deposited on spaces around the inducer's anchoring sites, causing a decrease in metallic particle sizes, as observed with XDR and TEM.

**Table 3**

Binding energies (eV) of internal electrons and atomic surface ratio of 1 wt% Pt/AlCD(x) catalysts.

Catalyst	Pt 4d <sub>5/2</sub> (eV)	N 1s (eV)	Al 2p (eV)	Pt/Al at	N/Al at	Pt/N at
1% Pt/AlCD(0)	315.0 (85) 317.0 (15)	—	74.5	0.0053	—	—
1% Pt/AlCD(1)	315.1 (77) 317.0 (23)	399.7 (56) 401.6 (44)	74.5	0.0074	0.021	0.35
1% Pt/AlCD(5)	315.0 (78) 317.0 (22)	399.8 (50) 401.8 (50)	74.5	0.0135	0.038	0.35
1% Pt/AlCD(10)	315.1 (74) 317.0 (26)	399.6 (52) 401.7 (48)	74.5	0.0141	0.049	0.29
1% Pt/AlCD(15)	315.0 (71) 317.0 (29)	399.5 (50) 401.6 (50)	74.5	0.0158	0.078	0.20
1% Pt/AlCD(20)	315.0 (70) 317.0 (30)	399.6 (54) 401.7 (46)	74.5	0.0171	0.109	0.16

### 3.3. Enantioselective hydrogenation of PPD

#### 3.3.1. TMS-CD effect

Fig. 6 shows the curves of catalytic activity. For all catalysts, the activity changed with the TMS-CD content in the support. A pseudo-first-order kinetics with respect to PPD was found in all cases, reaching conversion levels of over 90% at 240 min of reaction for the catalysts 1% Pt/AlCD(x) with  $5 < x < 10$  and under 90% for those of  $x = 1, 15$  and 20. Scheme 2 displays the hydrogenation reaction of the substrate in relation to the carbonyl groups. All the catalysts were enantioselective for (R)-1-hydroxy-1-phenylpropan-2-one (1R-PP) and (R)-2-hydroxy-1-phenylpropan-1-one (2R-PP). Products of over hydrogenation were not detected.

Pt/AlCD(0) had the smaller activity of all the catalyst tested, mostly due to the large Pt particle size. Previous studies by Margitfalvi et al. [11,35,36] suggest the formation of a weak complex between the adsorbed inducer and the substrate for those supported metallic catalysts where the inducer is added *in situ*. The catalysts supported on AlCD(x) with  $x \neq 0$  behave similarly. Table 4 shows the conversion levels and the rate pseudo-constants,  $k_g$ . Nevertheless, the higher than nominal C (%) for 1% Pt/AlCD(x) with  $x: 1\text{--}5$  indicates higher surface poisoning by impurities, but the catalysts show higher conversion levels. This suggests a change of metallic sites size that translates into better active site–substrate interactions during hydrogenation. A different trend was observed for catalysts 1% Pt/AlCD(x) with  $x: 15\text{--}20$ , these catalysts show a major TMS-CD anchoring, which caused a decrease in both  $S_{BET}$  and in the average metallic particle size (shown in Table 2). This TMS-CD increment had a major stabilization effect, generating smaller-sized nanoclusters. The pore volume showed a decrease of 1.0–1.3 nm (compared to unmodified support) that causes a decrease in catalytic activity by surface block of the active sites

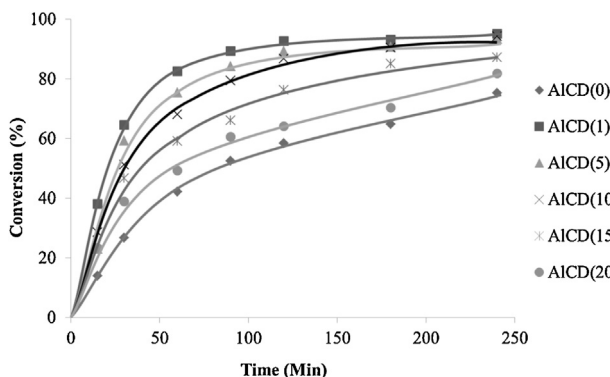


Fig. 6. Activity curves based on PPD for all the synthesized catalysts. Reaction conditions: PPD concentration: 0.01 mol/L, catalyst mass: 0.050 g,  $P_{H_2}$ : 40 bar, mixing speed: 700 rpm, solvent: cyclohexane.

located inside of the pores and/or by repulsive steric interactions with the immobilized inducer.

Fig. 7 shows the evolution of enantiomeric excess (ee) in function of conversion. All the catalysts were selective for the hydrogenation of the carbonyl groups (see Scheme 2). 1R-FP was the major reaction product, and the ee<sub>C1</sub> was similar to those reported for systems in which the chiral inducer was added *in situ* and acted adsorbed on the surface of the catalyst [37,38]. The most enantioselective catalyst was 1% Pt/AlCD(5) given an ee 44%. Table 4 shows the catalytic data for PPD hydrogenation on 1% Pt/AlCD(x) catalysts. All the catalysts showed hydrogenation of carbonyl of the acetyl group, with 2R-FP being the preferred product.

The rs values show high hydrogenation of the carbonyl adjacent to the phenyl group, with values of 46 for the catalyst 1% Pt/AlCD(0). This is due to the high adsorption capacity of the phenyl group of PPD at the active sites (for  $\eta$  bond formation between the active phase and the  $\pi$  aromatic cloud of the phenyl group) in line with studies by Toukoniitty et al. [39–43].  $\gamma$ -Al<sub>2</sub>O<sub>3</sub> have the ability to hydrogenate the carbonyl of acetyl groups as some researchers have reported [43,44]. This metal oxide possesses different types of acid-base sites on its surface which promotes the hydrogenation of non-planar groups by Lewis type interactions. The non-bonding electrons from the carbonyl group interact with the acidic sites of the support [45–47]. We found selectivity values similar to those reported by Toukoniitty et al. [40–43].

The polarization effect detected on surface Pt is attributed to both the chiral inducer and the support. We believe that this promotes the selectivity of the catalysts. In other studies [24] we have used SiO<sub>2</sub> as support, and we detected lower Pt<sup>0</sup>/Pt<sup>δ+</sup> ratios than those for  $\gamma$ -Al<sub>2</sub>O<sub>3</sub> at similar nominal contents of TMS-CD. The

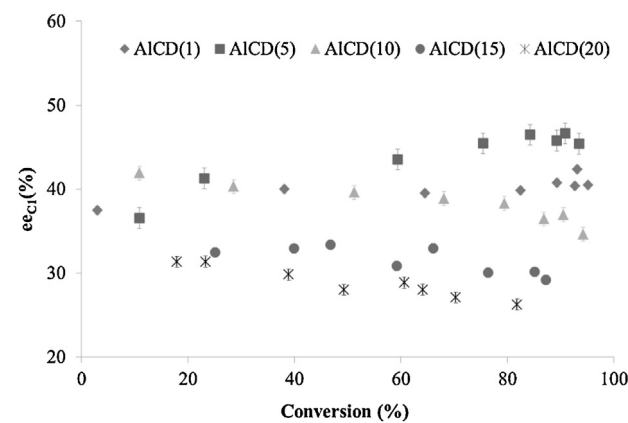
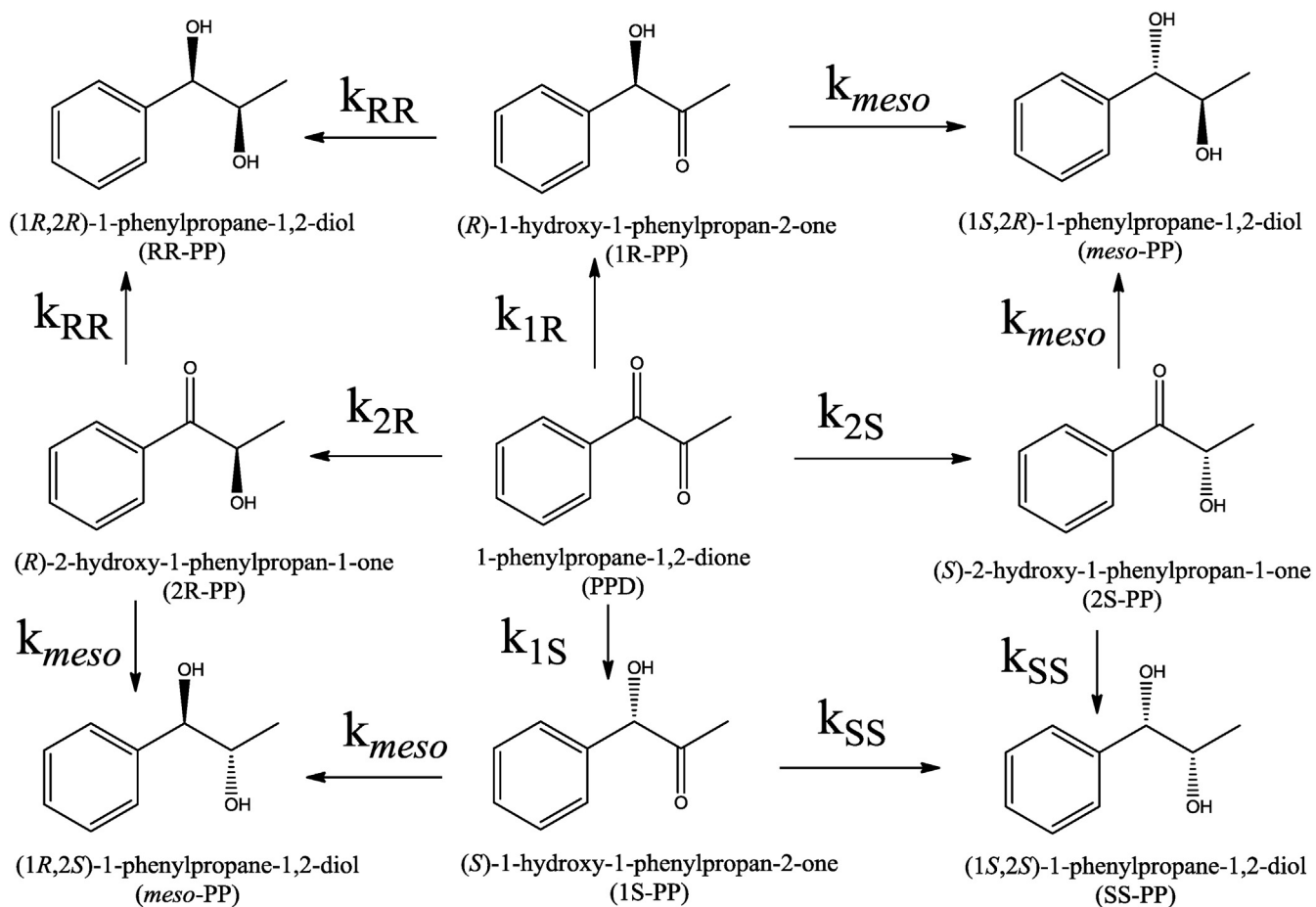


Fig. 7. Curves of enantiomeric excess in function of the conversion of PPD for all the synthesized catalysts on AlCD(x). Reaction conditions: PPD concentration: 0.01 mol/L, catalyst mass: 0.050 g,  $P_{H_2}$ : 40 bar, mixing speed: 700 rpm, solvent: cyclohexane.

**Scheme 2.** Hydrogenation route of 1-phenylpropane-1,2-dione.

increase in the polarization of Pt nanoparticles is attributed to the acidic characteristic of the Al species on the surface.

### 3.3.2. Effect of $H_2$ pressure

After finding the optimum catalyst system i.e., Pt/AlCD(5), the effect of  $H_2$  pressure over the enantiomeric excess was measured. These results are shown in Table 5. The surface  $H_2$  concentration may directly influence the adsorption of the reactant and thus enantioselectivity.  $H_2$  pressure increase (from 10 to 40 bar) had a marked effect on the conversion levels but only a discreet effect on the  $ee_{C1}$  value. The best  $ee_{C1}$  value was achieved at 40 bar, very similar as reported by Webb and Wells [48].

### 3.3.3. Effect of PPD concentration

Increasing liquid phase substrate concentrations lead to a significant effect on the catalytic behavior. The conversion and ee decreased with increasing the substrate/metal molar ratio keeping the catalyst mass constant. The conversion decreased drastically with further increase in the concentration of PPD, while only slight changes were seen in the ee (Table 6), which is similar to that reported for the hydrogenation of 3,5-bis(trifluoromethyl)acetophenone with Pt/Al<sub>2</sub>O<sub>3</sub> catalyst modified with cinchonidine (CD) [49]. The lowest conversion and ee were achieved at a 0.10 mol/L of PPD. The increase of PPD concentration should increase in the amount of substrate on the Pt surface. This

**Table 4**  
Catalytic data for PPD hydrogenation. Reaction conditions: PPD concentration: 0.01 mol/L,  $P_{H_2}$ : 40 bar, catalyst mass: 0.050 g and stirring speed: 700 rpm, solvent cyclohexane.

X	X ( $\pm 0.2\%$ )	ee <sub>C1</sub> ( $\pm 0.2\%$ )	ee <sub>C2</sub> ( $\pm 0.2\%$ )	rs	$k_g$ ( $\text{min}^{-1} \text{g}^{-1}$ )	$k_{1R}$ ( $\text{min}^{-1} \text{g}^{-1}$ )	$k_{1S}$ ( $\text{min}^{-1} \text{g}^{-1}$ )	$k_{2R}(10^3 \text{ min}^{-1} \text{g}^{-1})$	$k_{2S}(10^3 \text{ min}^{-1} \text{g}^{-1})$
0	75.4	1.3	1.0	46.2	0.160	0.078	0.078	1.69	1.69
1	95.1	40.2	14.3	63.8	0.536	0.372	0.157	4.26	3.21
5	93.2	44.6	17.8	134.9	0.438	0.315	0.118	2.73	2.36
10	94.3	38.2	17.5	108.6 <sup>a</sup>	0.318	0.217	0.101	—	—
15	88.4	31.5	16.2	106.4 <sup>a</sup>	0.243	0.156	0.087	—	—
20	81.3	29.0	17.0	97.5 <sup>a</sup>	0.224	0.144	0.080	—	—

Conversion (X) at 240 min of reaction. ee<sub>C1</sub> – ee<sub>C2</sub> and rs corresponds to the average values.

<sup>a</sup> Products determined to conversions above 120 min reaction unrepresentative in its contribution in  $k_g$  calculations.

**Table 5**

Catalytic data for PPD hydrogenation on 1% Pt/AlCD(5) catalyst at different H<sub>2</sub> pressures. Reaction conditions: PPD concentration: 0.01 mol/L, catalyst mass: 0.050 g and stirring speed: 700 rpm, solvent cyclohexane.

Pressure (bar)	X ( $\pm 0.2\%$ )	ee <sub>C1</sub> ( $\pm 0.2\%$ )	k <sub>g</sub> (min <sup>-1</sup> g <sup>-1</sup> )	k <sub>1R</sub> (min <sup>-1</sup> g <sup>-1</sup> )	k <sub>1S</sub> (min <sup>-1</sup> g <sup>-1</sup> )
0.5	87.3	39.3	0.206	0.144	0.062
10	91.5	43.2	0.246	0.176	0.069
20	92.2	44.0	0.332	0.234	0.098
40 <sup>a</sup>	93.5	44.6	0.438	0.317	0.118

Conversion (X) at 240 min of reaction, ee<sub>C1</sub> corresponds to the average values.

<sup>a</sup> More details in Table 4.

**Table 6**

Catalytic data for PPD hydrogenation on 1% Pt/AlCD(5) catalyst at different PPD concentrations. Reaction conditions: P<sub>H<sub>2</sub></sub>: 40 bar, catalyst mass: 0.050 g and stirring speed: 700 rpm, solvent cyclohexane.

Concentration (mol/L)	Mole rate FPD/Pt <sub>total</sub>	X ( $\pm 0.2\%$ )	ee <sub>C1</sub> ( $\pm 0.2\%$ )	k <sub>g</sub> (min <sup>-1</sup> g <sup>-1</sup> )	k <sub>1R</sub> (min <sup>-1</sup> g <sup>-1</sup> )	k <sub>1S</sub> (min <sup>-1</sup> g <sup>-1</sup> )
0.010 <sup>a</sup>	100	93.5	44.6	0.438	0.317	0.118
0.025	250	76.3	37.2	0.216	0.148	0.068
0.050	500	73.9	32.7	0.120	0.079	0.041
0.100	1000	62.8	33.6	0.088	0.060	0.028

Conversion (X) at 240 min of reaction, ee<sub>C1</sub> corresponds to the average values.

<sup>a</sup> More details in Table 4.

**Table 7**

Catalytic data for PPD hydrogenation on 1% Pt/AlCD(5) catalyst using different solvents. Reaction conditions: concentration of PPD 0.01 mol/L, P<sub>H<sub>2</sub></sub>: 40 bar, catalyst mass: 0.050 g and stirring speed: 700 rpm, solvent cyclohexane.

Solvent	$\epsilon^a$	X ( $\pm 0.2\%$ )	ee <sub>C1</sub> ( $\pm 0.2\%$ )	k <sub>g</sub> (min <sup>-1</sup> g <sup>-1</sup> )	k <sub>1R</sub> (min <sup>-1</sup> g <sup>-1</sup> )	k <sub>1S</sub> (min <sup>-1</sup> g <sup>-1</sup> )
Chloroform	1.10	64.5	14.9	0.134	0.097	0.036
Cyclohexane	2.02	93.5	44.6	0.548	0.385	0.163
Toluene	2.39	95.9	38.6	0.568	0.414	0.154
Ethyl acetate	6.11	84.0	35.3	0.360	0.246	0.114
THF	7.58	5.2	34.5	0.008	0.005	0.003
Ethanol	24.3	80.9	23.4	0.120	0.077	0.043

Conversion (X) at 240 min of reaction, ee<sub>C1</sub> corresponds to the average values.

<sup>a</sup> Values taken from Ref. [49].

coverage is responsible for the decrease of the conversion values. At concentrations of PPD higher than 0.01 mol/L hydrogenation of the acetyl group was not detected (Tables 4 and 6). The increment in the rs as the PPD concentration increases can be understood as follows: the active sites of the catalyst are saturated by the substrate at high PPD concentrations, promoting the co-planar adsorption of the substrate through the phenyl ring, and subsequently decreasing the hydrogenation of the acetyl group.

### 3.3.4. Effect of the solvent

The effect of different solvents on the catalytic behavior was studied. The results are displayed in Table 7. The dielectric constants of pure solvents were used excluding the effect of small amounts of reactant and anchored modifier. Hydrogenation kinetics in various solvents was described in terms of reaction rates, and enantioselectivity. Here we propose a qualitative model including enantioselectivity and the dielectric constant of the pure solvents, similar to that proposed by Toukoniity et al. [50].

As expected, the reaction rate varied with the different solvents. The highest reaction rate was observed in toluene and very low reaction rates were seen in chloroform and tetrahydrofuran (THF), while relatively high rates were obtained in the other solvents in this study. Toukoniity et al. [50] have reported that the initial hydrogenation rate did not correlate with the hydrogen solubility. We did not find a clear relation between the activity and dielectric constant.

The main effort of this work was to understand the variation of enantioselectivity in different solvents. The ee was almost 15% in chloroform and increased up to 40% in toluene. Fig. 8 shows a highly non-linear dependence of the ee on the dielectric constant of the solvent. Thus, cyclohexane and toluene display similar

conversions, a slight difference in ee<sub>C1</sub>, which we attributed to their similar  $\epsilon$  value, and to the strong interactions with the TMS-CD on the surface. The ee decreased as the solvent dielectric constant value increase, agreeing with those reported in literature [50].

### 3.4. Recycling

The catalyst supported on AlCD(5) presented the highest value of ee, and was selected as the model system for stability, activity, and selectivity assays in consecutive batch cycles. Between cycles, the catalyst was washed with chloroform in order to remove both the organic matter that could have been adsorbed on the support,

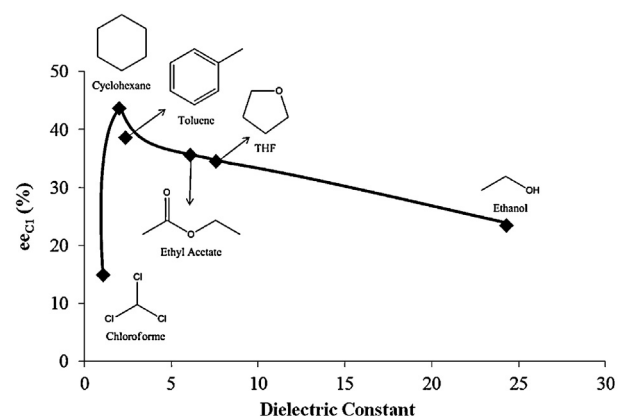


**Fig. 8.** Curves of enantiomeric excess in function of dielectric constant for PPD hydrogenation on 1% Pt/AlCD(5) at different solvents. Reaction conditions: PPD concentration 0.01 mol/L, P<sub>H<sub>2</sub></sub>: 40 bar, catalyst mass: 0.050 g and stirring speed: 700 rpm.

**Table 8**

EA and XPS data for recycles of the catalyst 1% Pt/AlCD(5). Reaction conditions: PPD concentration: 0.01 mol/L, catalyst mass: 0.050 g,  $P_{H_2}$ : 40 bar, stirring speed: 700 rpm.

Run	C (%)	H (%)	N (%)	TMS-CD (wt%)	Pt 4d <sub>5/2</sub> (eV)	N 1s (eV)	Pt/Al at	N/Al at	Pt/N at
1	2.16	1.12	0.22	3.1	315.0 (78) 317.0 (22)	399.8 (50) 401.8 (50)	0.0135	0.038	0.35
5	8.85	2.68	0.16	2.3	315.0 (77) 317.0 (23)	399.8 (69) 401.8 (31)	0.0117	0.012	0.97

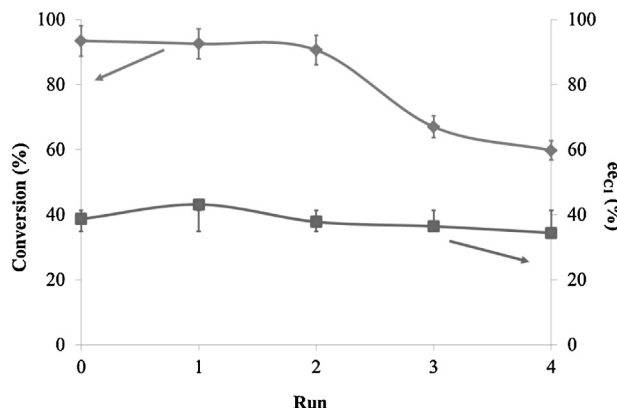


**Fig. 9.** Activity curves and ee in function of the number of reaction cycles for the catalyst 1% Pt/AlCD(5). Reaction conditions: PPD concentration: 0.01 mol/L, catalyst mass: 0.050 g,  $P_{H_2}$ : 40 bar, mixing speed: 700 rpm, solvent: cyclohexane.

and the TMS-CD from leaching [51]. **Table 8** shows the catalyst characterization after the last run. C (%) and H (%) were increased in the last cycle. This was attributed to the species formed on the surface of the support (hydroxyketones with Si—OH) which are of the type Si—O—R, as reported by Blümel [52] and/or to the presence of species heavily adsorbed from the substrate, products, and/or solvent. N (%) decreased with the cycles, assuming that leaching of the inducer takes place. XPS shows the presence of two types of surface nitrogen which are aliphatic (399.8 eV) and aromatic (401.8 eV) according to Gammon et al. [52]. The remaining anchored chiral inducer is slightly hydrogenated in the quinoline cycle of the TMS-CD as shown in **Table 8**, where the enhancement of the  $N_{\text{aliphatic}}/N_{\text{aromatic}}$  ratio was detected in agreement with previous studies performed by our group [24].

**Fig. 9** shows the variation of conversion and ee levels as a function of the number of reaction cycles. As the number of reaction cycle increased, the activity decreased, reaching values of 63% in the last run. Surface enrichment by undesired species on the support led to lower activity because they might be interfering in the adsorption of the substrate on the active sites. Subsequently, the hydrogenation at these sites produced a racemic mixture, decreasing the ee values.

Hydrogenation species of the carbonyl to the acetyl group were detected in each cycle, and the appearance of RR-diols, SS-diols, and meso diols. The preferred products in all cases were those with absolute R configuration, mainly 1R-FP. The catalyst selectivity decreased with the cycles for quinoline hydrogenation, and leaching of TMS-CD (increment in aliphatic N and N (%)) decrease as shown in **Table 8**.

#### 4. Conclusions

A catalyst system was synthesized for the enantioselective hydrogenation of PPD. Cinchonidine was tethered directly with prior silanization modification over activated  $\gamma\text{-Al}_2\text{O}_3$ . The supported metallic catalysts were obtained by the reduction of a metallic precursor undergoing  $H_2$  pressure. FTIR, TG/DTA and NMR data support the proposed immobilization. TEM images and XPS demonstrated that increasing cinchonidine content helps to homogenize Pt dispersion and size. 1% Pt/AlCD(x) catalyst systems

were tested for the desired reaction, and good ee value (44.0%) for  $x=5$  was found. Our study on the effect of the  $H_2$  pressure and PPD concentration in liquid phase indicated that the reaction conditions were very important in controlling the activity and enantioselectivity. All these are explained by the substrate adsorption on the active metal sites. The solvent effect studies showed non-linear correlation between enantiomeric excess and dielectric constant of the pure solvent. The most selective catalyst showed good reusability under optimum conditions.

#### Acknowledgements

Authors thank to CONICYT for financial support (FONDECYT GRANT 1061001) and to Red Doctoral REDOC.CTA. C.T. thanks to CONICYT for Doctoral Fellowship.

#### References

- [1] H.U. Blaser, B. Pugin, F. Spindler, *Applied Homogeneous Catalysis by Organometallic Complexes*, Weinheim, 1996.
- [2] J. Hagen, *Industrial Catalysis. A Practical Approach*, Alemania, 1999.
- [3] H.-U. Blaser, F. Spindler, M. Studer, *Appl. Catal. A: Gen.* 221 (2001) 119–143.
- [4] C. Chapuis, D. Jacoby, *Appl. Catal. A: Gen.* 22 (2001) 93–117.
- [5] T. Harada, Y. Izumi, *Chem. Lett.* 7 (1978) 1195–1196.
- [6] W.S. Knowles, *Angew. Chem. Int. Ed.* 41 (2002) 1998–2007.
- [7] E. Tálas, J.L. Margitfalvi, O. Egyed, *J. Catal.* 266 (2009) 191–198.
- [8] T. Burgi, A. Baiker, *Acc. Chem. Res.* 37 (2004) 909–917.
- [9] S.P. Griffiths, P. Johnston, P.B. Wells, *Appl. Catal. A: Gen.* 191 (2000) 193–204.
- [10] E. Schmidt, T. Mallat, A. Baiker, *J. Catal.* 272 (2010) 140–150.
- [11] J.L. Margitfalvi, E. Tálas, E. Tifirst, C.V. Kumar, A. Gergely, *Appl. Catal. A: Gen.* 191 (2000) 177–191.
- [12] K. Szőri, K. Balázsik, S. Cserényi, G. Szöllösi, M. Bartóka, *Appl. Catal. A: Gen.* 362 (2009) 178–184.
- [13] H.B. Wang, P.A. Wang, Q.J. Wang, X.L. Sun, L.L. Jing, *Chin. Chem. Lett.* 19 (2008) 1440–1444.
- [14] D.D. Vos, I.F.J. Vankelecom, P.A. Jacobs, *Chiral Catalyst Immobilization and Recycling*, Toronto, 2000.
- [15] Q.-H. Fan, Y.-M. Li, A.S.C. Chan, *Chem. Rev.* 102 (2002) 3385–3466.
- [16] A. Ghosh, R. Kumar, *J. Catal.* 228 (2004) 386–396.
- [17] C.E. Song, S.-G. Lee, *Chem. Rev.* 102 (2002) 3495–3524.
- [18] C.-H. Chu, E. Jonsson, M. Auvinen, J.J. Pesek, J.E. Sandoval, *Anal. Chem.* 65 (1993) 808–816.
- [19] N. Fukaya, H. Haga, T. Tsuchimoto, S. Onozawa, T. Sakakura, H. Yasuda, *J. Organomet. Chem.* 695 (2010) 2540–2542.
- [20] M.T. Matyska, J.J. Pesek, A. Katrekar, *Anal. Chem.* 71 (1999) 5508–5514.
- [21] J.J. Pesek, M.T. Matyska, E.J. Williamsen, M. Eavanchic, V. Hazari, K. Konjuh, S. Takhar, R. Tranchina, *J. Chromatogr. A* 786 (1997) 219–228.
- [22] J.J. Pesek, V.H. Tang, *Chromatographia* 39 (1994) 649–654.
- [23] J.E. Sandoval, J.J. Pesek, *Anal. Chem.* 61 (1989) 2067–2075.
- [24] C.H. Campos, M. Oportus, C. Torres, C. Urbina, J.L.G. Fierro, P. Reyes, *J. Mol. Catal. A: Chem.* 348 (2010) 30–41.
- [25] A. Roucoux, J. Schulz, H. Patin, *Chem. Rev.* 102 (2002) 3757–3778.
- [26] A. Lindholm, P. Mäki-Arvela, E. Toukoniitty, T.A. Pakkanen, J.T. Hirvi, T. Salmi, D.Y. Murzin, R. Sjöholm, R. Leino, *J. Chem. Perkin Trans. 12* (2002) 2605.
- [27] E. Toukoniitty, P. Mäki-Arvela, A.K. Neyestanaki, T. Salmi, R. Sjöholm, R. Leino, E. Laine, P.J. Kooyman, T. Ollonqvist, J. Väyrynen, *Appl. Catal. A: Gen.* 216 (2001) 73.
- [28] C.D. Wagner, L.E. Davis, M.V. Zeller, J.A. Taylor, R.H. Raymond, L.H. Gale, *Surf. Interf. Anal.* 3 (1981) 211.
- [29] J.J. Pesek, M.T. Matyska, A. Dabrowski, *Studies in Surface Science and Catalysis*, Elsevier, 1999, pp. 117–142.
- [30] J.J. Pesek, J.E. Sandoval, M. Su, *J. Chromatogr.* 630 (1993) 95–103.
- [31] A. Kurganov, U. Triidinge, T. Isaeva, K. Unger, *Chromatographia* 42 (1996) 217–222.
- [32] G. Corro, J.L.G. Fierro, V.C. Odilon, *Catal. Commun.* 4 (2003) 371–376.
- [33] D. Ruiz, J.L.F. Fierro, P. Reyes, *J. Braz. Chem. Soc.* 21 (2010) 262.
- [34] D. Ruiz, P. Reyes, *J. Chil. Chem. Soc.* 54 (2008) 1740.
- [35] J.L. Margitfalvi, E. Tálas, *Appl. Catal. A: Gen.* 301 (2006) 187–195.
- [36] J.L. Margitfalvi, E. Tifirst, *J. Mol. Catal. A: Chem.* 139 (1999) 81–95.
- [37] P. Reyes, T. Marzialetti, J.L.G. Fierro, *Catal. Today* 107–108 (2005) 235.
- [38] C. Urbina, G. Pecci, C. Campos, P. Reyes, *J. Chil. Chem. Soc.* 54 (2010).

- [39] I. Busygina, J. Wärnå, E. Toukoniitty, D.Y. Murzin, R. Leino, *J. Catal.* 254 (2008) 339–348.
- [40] E. Toukoniitty, S. Franceschini, A. Vaccari, D.Y. Murzin, *Appl. Catal. A: Gen.* 300 (2006) 147–154.
- [41] E. Toukoniitty, P. Mäki-Arvela, J. Wärnå, T. Salmi, *Catal. Today* 66 (2001) 411–417.
- [42] E. Toukoniitty, V. Nieminen, A. Taskinen, J. Päivärinta, M. Hotokka, D.Y. Murzin, *J. Catal.* 224 (2004) 326–339.
- [43] E. Toukoniitty, B. Ševčíková, P. Mäki-Arvela, J. Wärnå, T. Salmi, D.Y. Murzin, *J. Catal.* 213 (2003) 7–16.
- [44] V. Nieminen, A. Taskinen, M. Hotokka, D.Y. Murzin, *J. Catal.* 245 (2007) 228–236.
- [45] B.C. Lippens, J.H.D. Boer, *Acta Crystallogr.* 17 (1964) 1312–1321.
- [46] X. Liu, R.E. Truitt, *J. Am. Chem. Soc.* 119 (1997) 9856–9860.
- [47] C. Morterra, G. Magnacca, *Catal. Today* 27 (1996) 497–532.
- [48] G. Webb, P.B. Wells, *Catal. Today* 12 (1992) 319–337.
- [49] R. Hess, A. Vargas, T. Mallat, T. Bürgi, A. Baiker, *J. Catal.* 222 (2004) 117–128.
- [50] E. Toukoniitty, P. Mäki-Arvela, J. Kuusisto, V. Nieminen, *J. Mol. Catal. A: Chem.* 192 (2003) 135–151.
- [51] A. Vargas, T. Bürgi, A. Baiker, *J. Catal.* 226 (2004) 691–692.
- [52] J. Blümel, *J. Am. Chem. Soc.* 117 (1995) 2112–2113.